IOP Publishing and International Atomic Energy Agency Nuclear Fusion

Nucl. Fusion **49** (2009) 065031 (8pp) doi:10.1088/0029-5515/49/6/065031

Off-axis neutral beam current drive for advanced scenario development in DIII-D

M. Murakami[1,a], J.M. Park[1], C.C. Petty[2], T.C. Luce[2], W.W. Heidbrink[3], T.H. Osborne[2], R. Prater[2], M.R. Wade[2], P.M. Anderson[1], M.E. Austin[4], N.H. Brooks[2], R.V. Budny[5], C.D. Challis[6], J.C. DeBoo[2], J.S. deGrassie[2], J.R. Ferron[2], P. Gohil[2], J. Hobirk[7], C.T. Holcomb[8], E.M. Hollmann[9], R.M. Hong[2], A.W. Hyatt[2], J. Lohr[2], M.J. Lanctot[10], M.A. Makowski[8], D.C. McCune[5], P.A. Politzer[2], J.T. Scoville[2], H.E. St John[2], T. Suzuki[11], T.S. Taylor[2], W.P. West[2], E.A. Unterberg[12], M.A. Van Zeeland[2] and J.H. Yu[9]

[1] Oak Ridge National Laboratory, PO Box 2008, Oak Ridge, TN 37831, USA
[2] General Atomics, PO Box 85608, San Diego, CA 92186-5608, USA
[3] Department of Physics and Astronomy, University of California, Irvine, Irvine, CA 92697-4575, USA
[4] Fusion Research Center, University of Texas-Austin, Austin, TX, USA
[5] Princeton Plasma Physics Laboratory, Princeton, NJ, USA
[6] Euratom/UKAEA Fusion Association, Culham Science Centre, Abingdon, Oxon OX14 3DB, UK
[7] Max-Planck-Institut fur Plasmaphysik, IPP-EURATOM Association, Garching, Germany
[8] Lawrence Livermore National Laboratory, Livermore, CA, USA
[9] Center for Energy Research, University of California-San Diego, La Jolla, CA, USA
[10] Department of Applied Physics, Columbia University, New York, NY, USA
[11] Japan Atomic Energy Agency, Naka, Japan
[12] Oak Ridge Institute for Science Education, Oak Ridge, TN, USA

E-mail: murakami@fusion.gat.com

Received 30 January 2009, accepted for publication 21 April 2009
Published 26 May 2009
Online at stacks.iop.org/NF/49/065031

Abstract

Modification of the two existing DIII-D neutral beamlines is planned to allow vertical steering to provide off-axis neutral beam current drive (NBCD) peaked as far off-axis as half the plasma minor radius. New calculations for a downward-steered beam indicate strong current drive with good localization off-axis so long as the toroidal magnetic field, B_T, and the plasma current, I_p, point in the same direction. This is due to good alignment of neutral beam injection (NBI) with the local pitch of the magnetic field lines. This model has been tested experimentally on DIII-D by injecting equatorially mounted NBs into reduced size plasmas that are vertically displaced with respect to the vessel midplane. The existence of off-axis NBCD is evident in the changes seen in sawtooth behaviour in the internal inductance. By shifting the plasma upwards or downwards, or by changing the sign of the toroidal field, off-axis NBCD profiles measured with motional Stark effect data and internal loop voltage show a difference in amplitude (40–45%) consistent with differences predicted by the changed NBI alignment with respect to the helicity of the magnetic field lines. The effects of NBI direction relative to field line helicity can be large even in ITER: off-axis NBCD can be increased by more than 30% if the B_T direction is reversed. Modification of the DIII-D NB system will strongly support scenario development for ITER and future tokamaks as well as provide flexible scientific tools for understanding transport, energetic particles and heating and current drive.

PACS numbers: 52.55.Fa, 52.55.Wq, 52.50.Gj, 52.65.Pp, 52.55.Dy

(Some figures in this article are in colour only in the electronic version)

[a] Author to whom any correspondence should be addressed.

1. Introduction

Advanced tokamak (AT) research [1, 2] on DIII-D seeks to provide the scientific basis for steady-state, high-performance operation for ITER and future tokamak reactors. For steady-state operation, all of the plasma current must be driven noninductively (without a transformer). The leading approach to the steady-state scenario utilizes the naturally hollow profile caused by the bootstrap current [3], which results in a hollow current profile. Since the bootstrap current profile may not perfectly match the optimal current profile for high fusion performance, a flexible, localized and efficient source of noninductive current is needed for control. Experimentally, such high-performance discharges have been demonstrated on DIII-D; however, the duration is usually limited by the evolution of the current profile to an unstable state [4, 5]. Experimental measurements and simulations of these discharges have indicated that these discharges could be extended to near steady state if the current profile were maintained by replacing the remaining ohmic current (30–40%) near the half radius with externally driven current [6]. The needed off-axis current can be supplied by electron cyclotron current drive (ECCD) or by neutral beam current drive (NBCD) in the co-direction (i.e. CD in the same direction as the plasma current). The axial current can be supplied by a relatively small amount of on-axis NBCD and/or fast wave current drive (FWCD).

The most expedient solution to get substantial off-axis CD in DIII-D is to modify two of the four NB lines to allow vertical steering to drive current peaking as far off-axis as half the plasma radius. This capability should greatly increase the parameter space available for AT scenario development. However, experiments on ASDEX-U reported that observed current profiles deviate from the predicted ones even in the absence of MHD instabilities possibly due to redistribution of beam ions on a time scale shorter than the current redistribution time [7, 8].

New calculations for DIII-D indicate very good CD with good localization off-axis as long as the toroidal field, B_T, and plasma current, I_p, are in the same direction (for a beam steered downwards) [9]. The effects of the alignment of the neutral beam injection (NBI) relative to the magnetic field pitch can be large: for DIII-D the magnitude is 40% higher in the case with B_T and I_p in the same direction, and for ITER [10] it is up to 20%. This prediction has been tested successfully by off-axis NBCD experiments utilizing small cross-section plasmas that are vertically shifted, which places the peak deposition of the neutral beams near the mid-radius of the plasma. By shifting the plasma upwards or downwards, or by changing the sign of B_T, predicted differences in the off-axis NBCD profiles from the difference in magnetic alignment have been successfully validated against the measurements.

2. Evaluation of off-axis NBCD

DIII-D is equipped with four positive-ion-based neutral beamlines, with three co-injection and one counter-injection. Each beamline consists of two ion sources, with the more tangential left (LT) source aimed at the tangency radius of 1.17 m and the less tangential right (RT) source at the radius of 0.74 m for the co-beamlines, while the tangency radius is reversed for the LT and RT sources for the counter-beamline. The ion sources (48 cm high × 12 cm wide) operate at the nominal energy 75–81 keV, and inject about 2.3–2.5 MW of deuterium neutral beam power into the torus. The distance between the source and the intersection of the two beam optical axes at the midplane is 5.5 m [11].

Modification of the present NBI to provide off-axis NBCD should have the following objectives: (1) be capable of generating a significant amount of off-axis ($\rho \approx 0.5$) CD with reasonable localization; (2) retain the present on-axis NBI capability; (3) minimize the complexity of the modifications, e.g. by limiting the motion to one plane (vertical) and (4) be applicable to a wide range of operating parameters (e.g. at higher density). We plan to steer the beamline by raising the source end by up to 1.5 m (which inclines the beamline optical axis up to ≈15° downwards through the midplane vessel port) while retaining the present beamline components [12].

Orbit-following Monte-Carlo calculations were carried out using the NUBEAM module [13] in the TRANSP [14] and ONETWO [15] transport codes to evaluate the performance of the planned off-axis NBCD system [9]. Two different discharge conditions were chosen from DIII-D AT experiments: a low-density discharge (shot 111221) [6], with line-average density $\bar{n}_e = 4.2 \times 10^{19}\,\mathrm{m}^{-3}$, toroidal magnetic field $B_T = 1.91$ T, plasma current $I_p = 1.19$ MA, safety factor at 95% poloidal flux surface $q_{95} = 5.0$ and normalized beta $\beta_N = 3.4$; and a high-density discharge (shot 122976) [16] with $\bar{n}_e = 6.2 \times 10^{19}\,\mathrm{m}^{-3}$, $B_T = 1.74$ T, $I_p = 1.34$ MA, $q_{95} = 5.0$ and $\beta_N = 4.0$. Figure 1 shows the calculated profiles of off-axis NBCD for the low-density case for the left and right sources in the positive B_T direction.

The peak CD location moves off-axis from $\rho = 0$ to 0.45 as the beamline source height (Z_s) is raised by 1.5 m. Although the peak driven current density decreases by about a factor 2 when Z_s is increased from 0 to 1.5 m, the net NB driven current stays constant or somewhat increases. Both the peak and the total driven current values are about a factor of 2 higher for the more tangential left source, with similar dependences on Z_s, compared with the right source.

The characteristics of off-axis NBCD are sensitive to alignment of NBI with local pitch of the magnetic field line. For the co-injection case (and thus I_p in the positive direction), the beam from the left source in the positive toroidal field (B_T) direction yields the most favourable performance. Figure 2 shows calculated NBCD profiles for the positive and negative B_T directions. The positive B_T direction (the favourable alignment) case yields a profile of NBCD that is peaked off-axis at $\rho = 0.45$ and reasonably localized, while the negative B_T direction (the unfavourable alignment) case yields a broader profile with a peak near $\rho = 0.3$. The magnitude of the current is 40% higher in the case with the favourable alignment. Here the sign conventions for B_T and I_p are that the positive direction is counter clock-wise looking from the top of the tokamak.

The large differences in off-axis NBCD between the favourable and the unfavourable magnetic geometry are due primarily [9] to differences in: (a) fast ion trapping fraction and (b) electron shielding (cancellation) current which decreases with radius due to trapping of electrons. The downward and tangentially steered beam is aligned better with the magnetic

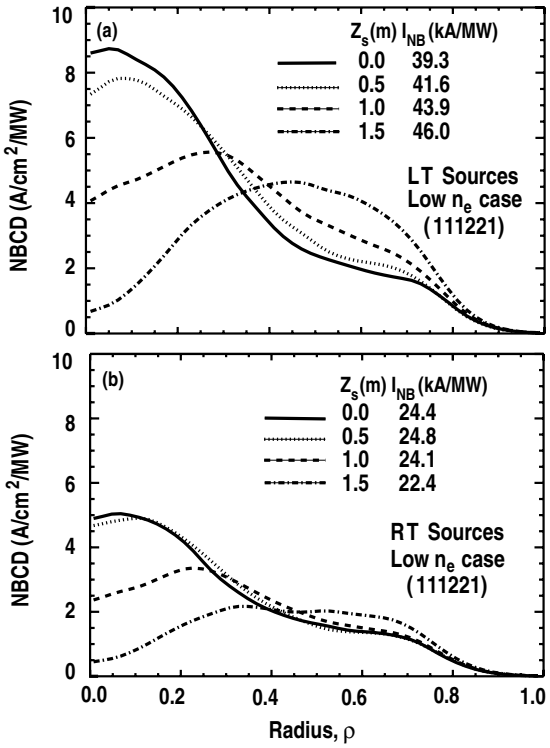

Figure 1. Calculated current density for off-axis co-NBCD, for the low-density discharge 111221, for (*a*) left (LT) beam and (*b*) right (RT) beam, each in four different steering angles from the source elevations of 0 cm (solid), 50 cm (dotted), 100 cm (dashed) and 150 cm (dot–dash).

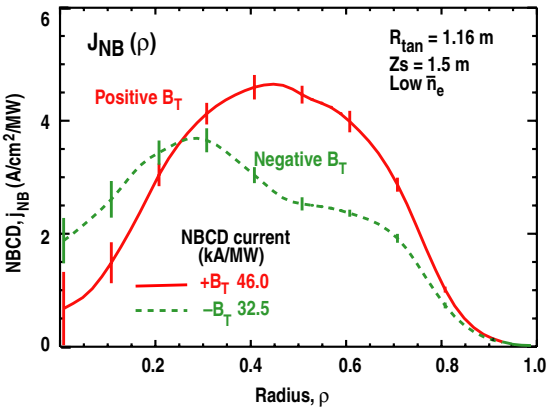

Figure 2. NBCD profiles for the positive (solid line) and negative (dashed line) B_T directions for the left (tangential) source only. The left beam in the positive B_T direction has the most favourable off-axis CD, while the off-axis feature is significantly lost for the left beam in the negative B_T direction.

field line pitch for the positive B_T direction than for the negative B_T (figure 3). Figure 4 shows illustrative examples of two early slowing down ('prompt') guiding centre orbits. The beam ions in the positive B_T direction stay in passing particle orbits, achieving well-localized off-axis CD. The same beam, but with B_T in the negative direction, has a larger pitch angle causing more trapped particle orbits and reducing the parallel ion current off-axis. The ion trapped fraction ($f_{i,trap}$) at the mid-radius in the unfavourable geometry is substantially larger than that in the favourable geometry as seen in figure 5(*a*).

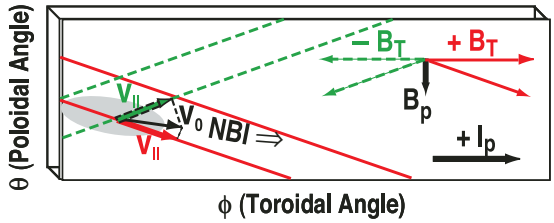

Figure 3. Beam injection projected onto the magnetic field line, for the positive (solid lines) and negative (dashed lines) toroidal field directions. The three arrows represent the beam on velocity (V_o) and its parallel velocity components projected to the magnetic field line for the positive and negative B_T case. (Reprinted courtesy of ANS, M. Murakami 2008 *Fusion Sci. Technol.* **54** 994)

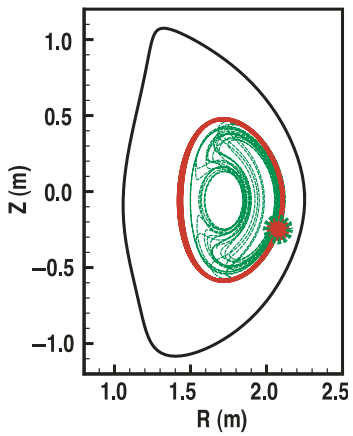

Figure 4. Examples of guiding centre drift orbits for (favourable alignment) $+B_T$ (solid lines) and (unfavourable alignment) $-B_T$ (dashed line) cases at the same birth locations during the early part of the slowing down processes. While the fast ion in the positive B_T direction stays in passing particle orbits, the ion in the negative B_T direction undergoes trapped particle orbits.

As slowing down and pitch angle scattering occur, $f_{i,trap}$ settles down to ≈20% and ≈10% for the unfavourable and the favourable geometry, respectively (figure 5(*a*)), affecting the fast ion current source. The guiding centre drift orbit shift of the trapped ions is larger by a factor of $(2R/r)^{1/2}$ than that of the passing fast ions. In particular, trapped particles whose guiding centres pass near the magnetic axis have large banana width, resulting in larger fast ion density near the axis, as seen in figure 4. Passing fast ions can more effectively build up fast ion current because they circulate more frequently around the torus than the trapped particles [17]. This leads to a substantial difference (by 25%) in fast ion current sources (figure 5(*c*)).

The net NBCD should include the 'shielding' current due to electrons that are collisionally dragged along with the circulating fast ions, as characterized by the shielding factor (figure 5(*d*)), the ratio of the net current drive to fast ion current. Since trapped electrons do not participate in cancellation of the fast ion current, the increase in the trapped electron fraction with radius results in increasing the relative difference to 30% in the net NBCD between the favourable and the unfavourable configuration, as seen in figure 2. In the favourable configuration, the NBCD efficiency does not decrease with radius. This is not the case for ECCD in which the radial increase in trapped electron population is detrimental.

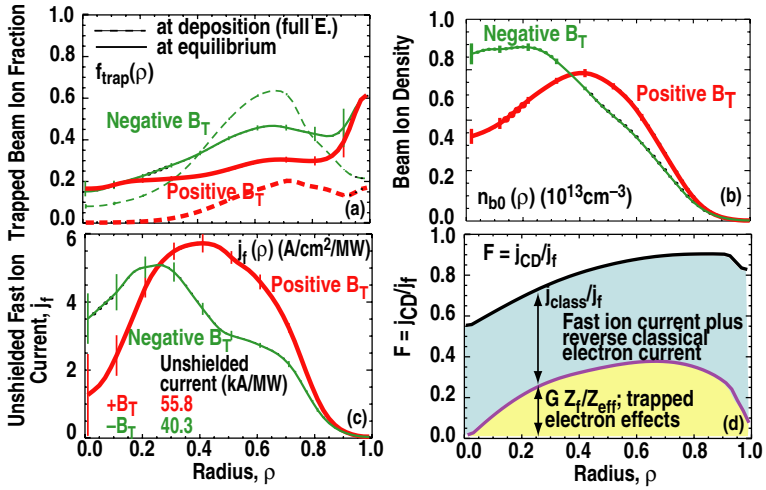

Figure 5. Fast ion trapping fraction for the favourable (bold line) and the unfavourable (fine line) alignment cases: (*a*) at deposition and at equilibrium, (*b*) beam ion density profiles, (*c*) profiles of the unshielded fast ion current and (*d*) profile of the shielding factor, composed of classical contribution and trapped electron contribution.

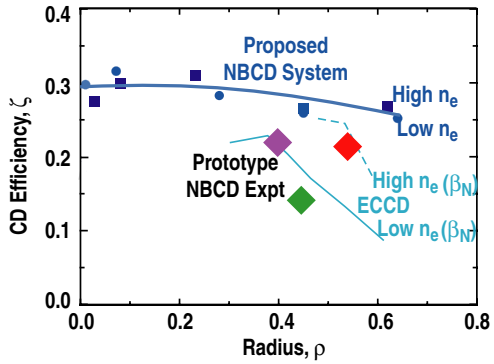

Figure 6. Dimensionless CD efficiencies calculated for the off-axis NBCD (small symbols) and the present off-axis NBCD experimental measurements (large symbols) and off-axis ECCD (lines) as functions of peak CD radius on DIII-D. The ECCD efficiencies were calculated for the two discharge conditions using TORAY-GA.

Because of these considerations off-axis NBCD does not lose CD efficiency at larger radius. Figure 6 shows the dimensionless CD efficiency as a function of the peak CD location. The dimensionless CD efficiency [18] is defined:

$$\xi = \frac{e^3}{\varepsilon_0^2}\left(\frac{IRn_e}{\mathrm{PkT_e}}\right) = 33\frac{I(\mathrm{A})R(\mathrm{m})n_e(10^{20}\,\mathrm{m}^{-3})}{P(\mathrm{W})T_e(\mathrm{keV})}. \quad (1)$$

The particular normalized CD efficiency is convenient to compare with ECCD efficiency which isolates the radial dependence of electron trapping effects. For the NBCD case, the radial dependence comes from the electron shielding effect.

The ECCD efficiencies in figure 6 are calculated for the profiles of the two discharges using the TORAY-GA code [19]. As expected, the ECCD efficiency is higher for the higher β discharge, but the accessible radial range is reduced due to refraction near the high-density cutoff. In comparison with the ECCD efficiency, the off-axis NBCD efficiency is somewhat better under the same conditions. Equally important is the fact that it does not decrease as much with radius. The normalized efficiencies of the prototype off-axis NBCD experiment are also shown in the figure.

The best NBCD does not necessarily imply the best fast ion confinement. As discussed, the best off-axis NBCD requires good off-axis CD localization and good shielding factor (F = net NBCD/fast ion current). The best fast confinement may follow from the large concentration of fast ions near the axis in the unfavourable alignment case. The large shift towards the axis (as seen in figure 4) reflects better fast ion performance (e.g., neutron emission rate) in the unfavourable alignment case, even though the total number of fast ions is the same. In the low-density case, the calculated neutron rate is higher by ∼10% for the unfavourable alignment case than the favourable alignment case.

3. Prototype off-axis NBCD experiment

A prototype off-axis NBCD experiment was performed on DIII-D to validate the magnetic alignment model. The experiment had three specific objectives: (1) to demonstrate that off-axis NBCD could be generated efficiently; (2) to validate the magnetic field alignment model and (3) to study the effects of anomalous fast ion transport on off-axis NBCD. Off-axis NBCD was achieved with the existing DIII-D midplane neutral beam injectors by utilizing small-size plasmas that are vertically shifted, placing the peak deposition of the neutral beams near the half radius of the plasma. The predicted magnetic field alignment effect could be tested by changing the sign of B_T or reversing the vertical offset position (figure 7(*a*)), which results in reversing the poloidal field (B_p) direction with respect to the beam injection velocity, thereby changing the alignment (figure 7(*b*)) between NBI and magnetic field lines. It should be noted that injection into the upward shifted ($+Z_0$) plasma by the present DIII-D NBI system corresponds to 'downward steering' of beam injection in full-sized unshifted discharge; positive B_T and positive I_p generate favourable alignment.

In addition to the discharge flexibilities needed for such tests, DIII-D has an excellent diagnostic set for studying off-axis NBCD, including motional Stark effect (MSE) polarimetry [20] to measure the magnetic pitch angles and

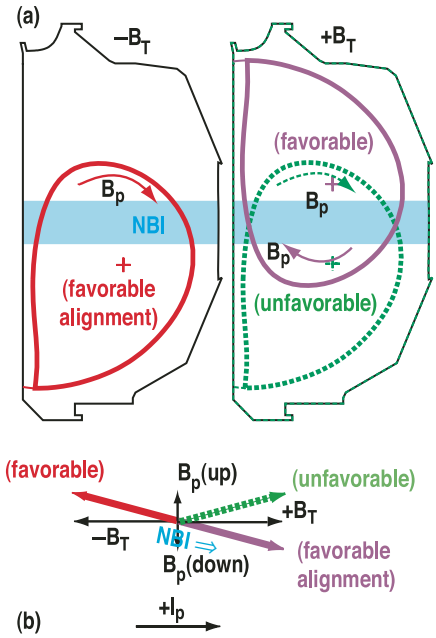

Figure 7. (*a*) Geometry of the prototype off-axis NBCD experiment, which tested the magnetic alignment model by changing B_T and vertical shifting the plasma centre (resulting in reversing the poloidal field direction); (*b*) vector diagram for beam injection parallel to or slightly across the magnetic field line, depending on the positive (solid line) and negative (dashed line) toroidal field direction.

multiple fast ion D_α (FIDA) spectroscopy views [21] and a 2D FIDA imaging system [22] to measure the beam ion density profiles. The MSE and FIDA spectroscopies are located near the vessel midplane where the neutral injectors are, so the major analysis challenge is to minimize unavoidable uncertainties due to limited diagnostic data inside $\rho \approx 0.4$ when the plasma is vertically shifted. For this reason, the vertically shifted phase of each discharge was followed by a swift (within 50 ms) shift back to the midplane to obtain better diagnostic information. The transition time (≈50 ms) is a factor of 2 shorter than the energy confinement time and the thermalization time of the full energy fast ions. Further experimental details will be discussed in [23].

The global behaviour of vertically shifted plasmas with off-axis NBI suggests the presence of off-axis CD that increased with co-NB power. Compared with a similar discharge kept at the midplane throughout the discharge, sawteeth were absent in soft x-ray and ECE data, and sawteeth reappeared well after shifting back to on-axis NBI in the down-shifted discharges with high enough NBI power and positive B_T (favourable alignment). The internal inductance decreased with increasing NBI power in shifted plasmas NBCD geometry, as expected from off-axis NBCD. Although these changes in the global parameters are consistent with the presence of off-axis current drive, they are not sufficient to prove the off-axis NBCD, since background discharge characteristics change as NBI goes from on-axis to off-axis. More convincing are the direct MSE measurements of the current profiles and fast ions (FIDA) during the off-axis NBCD phase, and comparison with the modelling under the experimental conditions.

Current drive profiles were determined from the 'loop-voltage analysis' [24] during both the on- and off-axis NBI phase. The analysis is based on time derivatives of MSE-based equilibrium reconstructions and conductivity profile measurements. The CD profile analysis benefited from differential CD analysis by taking differences in the loop voltages and MSE pitch angles [25] for two discharges with co- and balanced NBI with similar density, temperature and β (figure 8(*a*)). The systematic sources of error (e.g. $Z_{\rm eff}$) tend to cancel out in such an analysis. As shown in figure 8(*b*), even if we assume a systematic 30% error in the $Z_{\rm eff}$ profile, the difference in the current density between the co- and balanced injection does not change significantly and shows excellent agreement with the NUBEAM calculation. The difference also cancels out the sensitivity to the bootstrap current model.

The prediction that off-axis NBCD depends on the magnetic field alignment was validated by this experiment. Significantly greater (by ∼40%) NBCD was found in cases where the favourable alignment was used (that is both the upward-shifted positive B_T and the downward-shifted negative B_T) compared with the unfavourable alignment (the downward-shifted positive B_T cases), as shown in the NBCD profiles (figure 9(*a*)) and the NBCD integrated over $\rho = 0.4$–1.0 (figure 9(*b*)).

The MSE pitch angle measurements were in good agreement with MSE signals predicted by TRANSP simulations (figure 10) during off-axis NBCD. In MSE analysis and simulations, in order to reduce the systematic errors, the calibrations of the individual channels were adjusted to agree with calculated pitch angles including the radial electric field effects (E_r, based on the force balance calculation) at an early time in another shot. MSE simulations reproduced the MSE signals throughout the discharges, including the large excursion of the vertical shift back to the midplane. Agreement was best with MSE simulations which included no fast ion diffusion during off-axis NBCD with shifted plasmas, as shown in figure 10(*b*). However, MSE simulations during and after returning to on-axis NBCD appeared to be in better agreement with a modest *ad hoc* diffusion ($D_b < 0.3$—$0.5\,m^2\,s^{-1}$) included.

4. Implications of the magnetic alignment for off-axis NBCD in tokamaks

Off-axis NBCD is observed even with anomalous fast ion diffusion, especially for the favourable alignment cases. While the measured off-axis NBCD is observed to increase approximately linearly with injected power up to 7 MW, the calculated current tends to increase more strongly than linear. Addition of a modest amount of fast ion diffusion ($D_b < 0.5\,m^2\,s^{-1}$) is needed to explain an observed difference in the NBCD profile between measurement and the calculation at high power ($P_b > 5$ MW). However, there is no evidence that the off-axis is more prone to anomalous fast ion transport than on-axis NBCD. The results of the power scan data (up to 7.2 MW) will be reported elsewhere [23]. Analysis of data from the fast ion D_α diagnostics yields a similar conclusion which will be discussed elsewhere [26].

Fast ion diffusion moves off-axis particles towards the axis, in a manner similar to that of the geometry effect in the unfavourable alignment geometry. Modelling with an *ad hoc*

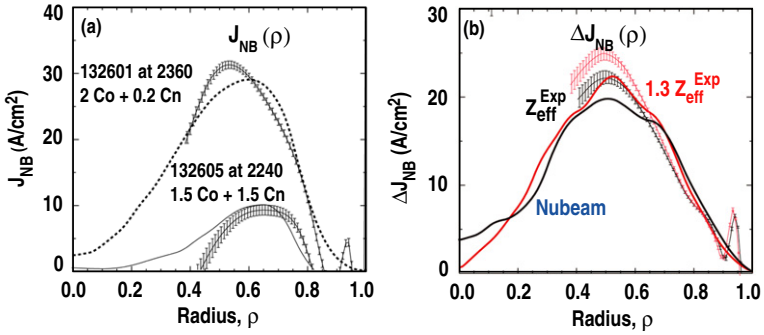

Figure 8. (*a*) NBCD analysis for co- and balanced NBI discharges, (*b*) difference in NBCD profiles for co- and balanced injection for the shift down with negative B_T case. The curves with random error bars are measurements and the curves without error bars are NUBEAM modelling.

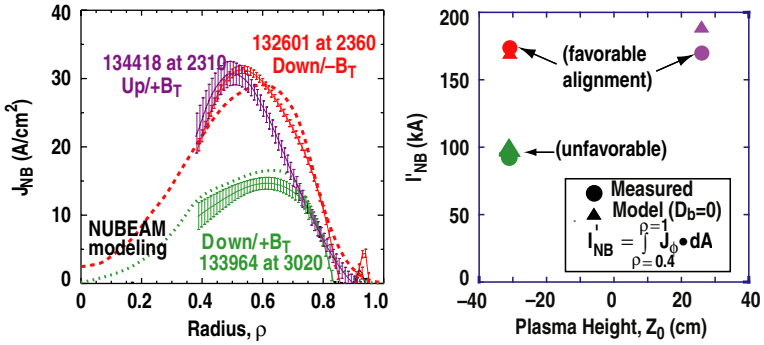

Figure 9. (*a*) Profiles of NBCD (measurements and modelling (dashed line)) and (*b*) NBCD integrated over the outer 60% radius as a function of vertical plasma position for three different configurations.

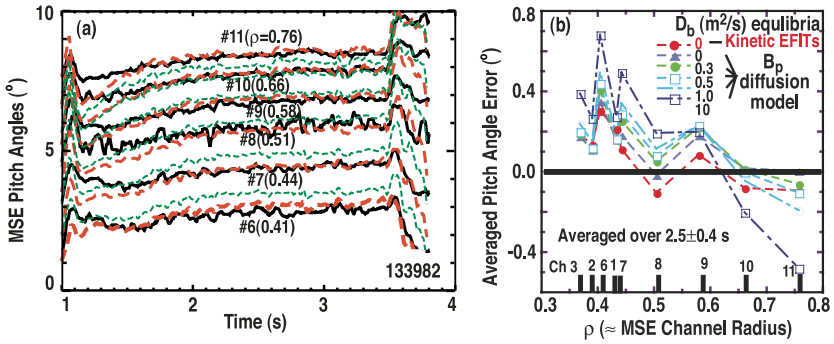

Figure 10. (*a*) Comparison between MSE measurements (solid line) and simulated signals without fast ion diffusion (long dashed line) and with diffusion coefficient 10 $m^2\,s^{-1}$ (short dashed lines) and (*b*) root-mean-square errors (between the measured and the simulated pitch angles) averaged over 400 ms for different fast ion diffusion assumptions, showing that the best agreement is without diffusion.

diffusion model shows (figure 11) that, to first approximation, off-axis peaking remains, and integrated current decreases in a similar way for both the favourable and the unfavourable cases. As for the application to AT plasmas, the effect of a modest amount of fast ion diffusion is not severe.

The magnetic alignment effects are important for interpreting off-axis NBCD experiments in tokamaks. ASDEX-U, JT60-U and JET all have pairs of upward- and downward-steered NB sources. Based on the above arguments, one source of the pair can produce better-localized off-axis NBCD with a larger amplitude, while the other source produces more diffused, smaller NBCD, depending on the relative directions of B_T and the beamline (I_p) direction. In the DIII-D case, all sources in the two planned beamlines are downward steered. DIII-D has sufficient flexibility to choose the B_T direction to optimize off-axis NBCD.

A ∼20% increase in off-axis NBCD is calculated for ITER, if it is operated in the reverse B_T direction. ITER will have an off-axis NB system, planned with downward steering of the beams and an upward-shifted plasma. Since ITER operates with both the B_T and I_p directions opposite to DIII-D's favourable direction, the downward-steered beam in the planned configuration is less favourable for off-axis NBCD. Figure 12 shows the NBCD profiles calculated for the positive B_T direction as well as the negative B_T direction in ITER for the maximum steering in the 2007 design (downward angle of 2.981°) and the 2001 EDA designs (3.365°) [26]. Negative B_T, which is not allowed operationally, has a larger

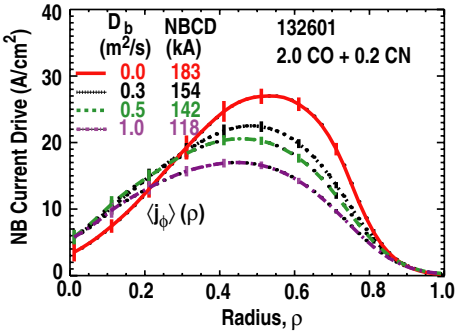

Figure 11. Effects of *ad hoc* fast ion diffusion on off-axis NBCD profiles for the low-density case, using the planned downward steering of the NBI of figure 2. Here B_T is positive and 2.0 co-NBI plus 0.2 counter-NBI beams are used.

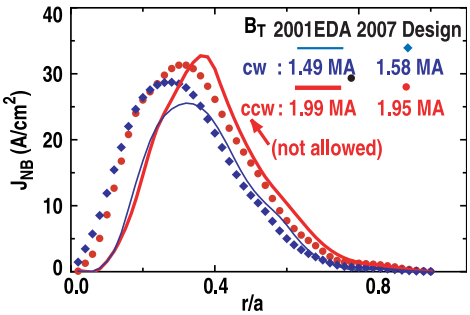

Figure 12. Calculated off-axis NBCD for both positive and negative (planned) B_T direction in the 2007 design of ITER for the maximum downward steering in the 2001 EDA (solid curves) and the 2007 (diamond, circles) designs. The negative B_T direction (bold curve), which is not allowed operationally, has a larger peak CD radius with 33% larger driven current.

peak CD radius (0.1 in ρ) with a larger (33%) driven current. Since the steady-state scenario requires the largest possible CD and the NB is the largest CD source, it is highly desirable to operate B_T in the negative direction. The recent design guideline is the wider steering angle, similar to the '2001 EDA' design, allowing more off-axis NBCD, even though with the unfavourable alignment [27].

5. Scenario development using the off-axis NBCD in DIII-D

Off-axis NBCD enables advanced scenario development in DIII-D. The main focus for steady-state scenario development in DIII-D is the demonstration of fully noninductive current sustainment for more than twice the current relaxation time ($\tau_R \sim 2$ s) at progressively higher pressures to meet the requirements of ITER and future tokamak reactors. DIII-D experiments have demonstrated stationary performance for about one τ_R at the normalized fusion performance using confinement scaling factor H_{89}, $G = \beta_N H_{89}/q_{95}^2 = 0.3$ which is sufficient to meet the ITER physics objective for steady-state operation, for a lower B_T (1.8 T) [6]. Demonstration at higher B_T (2.2 T) to better simulate future tokamak reactors requires a significant increase in power to drive off-axis current, which could be supplied by additional ECCD, or, alternately, off-axis NBCD using vertical steering.

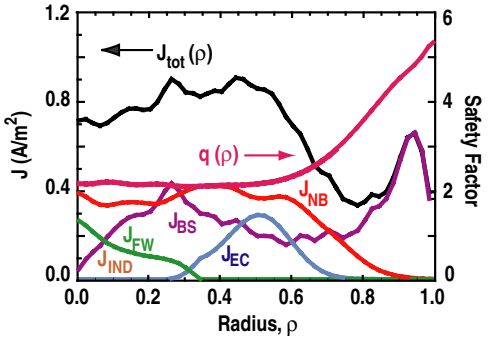

Figure 13. Profiles of current components and safety factor in a self-consistent GLF-23 simulation using off-axis NBCD for an ITER steady-state demonstration shot in DIII-D. Current densities shown are total (J_{TOT}), NBCD (J_{NB}), bootstrap current (J_{BS}), ECCD (J_{EC}), FWCD (J_{FW}) and inductive (J_{IND}).

High q_{min} scenario development at high β_N is limited at present by overdrive of the central current by the NBI that is required for heating. In scenario modelling of the $B_T = +1.8$ T case using the hardware proposed, the combination of off-axis NBCD (10 MW off-axis together with 5 MW on-axis) and high-power ECCD (4.5 MW) leads to a fully noninductive high-β scenario with flat $q(\rho)$ above 2 (figure 13). Off-axis NBI provides a broad CD needed at mid-radius that would not be possible with on-axis NBI alone (15 MW total) without over-driving the current near the axis. High-power ECCD affords detailed tailoring of the current profile for better stability and transport control. These scenario simulations were carried out with scaled experimental transport and a theory-based transport (GLF23) model in the ONETWO transport code.

6. Conclusion

The prospect for off-axis NBCD in DIII-D to supply a substantial amount of off-axis current drive needed for development of steady-state, advanced tokamak scenarios has been studied. Sensitivity of the magnitude and localization of off-axis NBCD to the beam injection relative to the magnetic pitch has been validated in the DIII-D prototype experiment. The measured off-axis NBCD profiles are consistent with predicted differences (40–45%) arising from the NBI orientation with respect to the magnetic field lines. The effect is large: ITER off-axis NBCD can be increased by ~20% if the direction of B_T is reversed. The effect is important to interpret the results of off-axis NBCD experiment in present tokamaks. Modification of the DIII-D NB system will strongly support scenario development for ITER and future tokamak reactors and will provide flexible scientific tools for understanding transport, energetic particles, heating and CD physics.

Acknowledgments

This work was supported by the US Department of Energy under DE-AC05-00OR22727, DE-FC02-04ER54698, SC-G903402, DE-FG03-97ER54415, DE-AC02-76CH03073, DE-AC52-07NA27344, DE-FG02-07ER54917, DE-FG02-89ER53297 and DE-AC05-06OR23100. The authors

acknowledge useful discussions with Drs D.N. Hill, A.G. Kellman and T. Oikawa. Some of the modelling was carried out using Grid-enabled TRANSP on the National Fusion Grid, and they would like to thank the National Fusion Collaboratory Project (www.fusiongrid.org) sponsored by the US DOE SciDAC Program.

References

[1] Taylor T.S. 1997 *Plasma Phys. Control. Fusion* **39** B47
[2] Luce T.C. 2005 *Fusion Sci. Technol.* **48** 1212
[3] Bickerton R.J, Connor J.W. and Taylor J.B. 1971 *Nature (London) Phys. Sci.* **229** 110
[4] Wade M.R. *et al* 2003 *Nucl. Fusion* **43** 634
[5] Murakami M. *et al* 2005 *Nucl. Fusion* **45** 1419
[6] Murakami M. *et al* 2006 *Phys. Plasmas* **13** 056106
[7] Hobirk J. *et al* 2004 *Proc. 30th EPS Conf. on Control. Fusion and Plasma Physics (St Petersburg, Russia, 2004)* Paper O-4.1B and http://epsppd.epfl.ch/StPetersburg/html/cidx0.html
[8] Günter S. *et al* 2007 *Nucl. Fusion* **47** 920
[9] Murakami M., Park J.M., Luce T.C., Wade M.R. and Hong R.M. 2008 *Fusion Sci. Technol.* **54** 994
[10] Shimomura Y., Murakami M., Polevoi A.R., Barabaschi P., Mukhovatov V. and Shimada M. 2001 *Plasma Phys. Control. Fusion* **43** A385
[11] Hong R., Colleraine, A.P., Haskovec J.S., Kellman D., Kim J., Nerem A., Phillips J.C., Sleaford B., Wight J.J. and Vella M.C. 1987 *Proc. 12th Symp. on Fusion Engineering (Monterey, CA, USA, 1987)* vol 2 (Piscataway, NJ: IEEE) p 1133
[12] Project Staff 2008 Five-Year Plan: 2008–2013 *General Atomics Report* GA-A25889, San Diego, CA http://web.gat.com/pubs/all.php?title=&p_author=&author=&meeting=&category=&date_from=&date_to=&mdate_from=&mdate_to=&Citation=&doc_num=A25889&formsubmit=Search
[13] Pankin A., McCune D., Andre R., Bateman G. and Kritz A. 2004 *Comput. Phys. Commun.* **159** 157
[14] Hawryluk R.J. 1980 *Physics Close to Thermonuclear Conditions* vol 1 (Brussels: Commission of the European Communities) p 19
[15] St John H.E., Taylor T.S., Lin-Liu Y.R. and Turnbull A.D. 1995 *Proc. 15th Int. Conf. on Plasma Physics and Controlled Nuclear Fusion Research 1994 (Seville, 1994)* vol 3 (Vienna: IAEA) p 603
[16] Garofalo A.M. *et al* 2006 *Phys. Plasmas* **13** 056110
[17] Wesson J. 1997 *Tokamaks* section 3.13 (Oxford: Oxford University Press) and references therein
[18] Luce T.C. *et al* 1999 *Phys. Rev. Lett.* **83** 4550
[19] Lin-Liu Y.R., Chan V.S. and Prater R. 2003 *Phys. Plasmas* **10** 4064
[20] Rice B.W., Burrell K.H., Lao L.L. and Lin-Liu Y.R. 1997 *Phys. Rev. Lett.* **79** 2694
[21] Heidbrink W.W., Burrell K.H., Luo Y., Pablant N. and Ruskov E. 2004 *Plasma Phys. Control. Fusion* **46** 1855
[22] Van Zeeland M.A., Heidbrink W.W. and Yu J.H. 2009 *Plasma Phys. Control. Fusion* **51** 055001
[23] Park J.M. 2009 Validation of on- and off-axis neutral beam current drive against experiment in DIII-D *Phys. Plasmas* submitted
[24] Forest C.B. *et al* 1997 *Phys. Plasmas* **3** 2846
[25] Petty C.C. 2005 *Fusion Sci. Technol.* **48** 1159
[26] Heidbrink W.W., Park J.M., Murakami M., Petty C.C. and Van Zeeland M.A. 2009 Observation of fast-Ion transport by microturbulence *Phys. Rev. Lett.* submitted
[27] Oikawa T. 2008 private communication